Research Article

A Hybrid Single-Carrier/Multicarrier Transmission Scheme with Power Allocation

Danilo Zanatta Filho,[1] Luc Féty,[2] and Michel Terré[2]

[1] *Signal Processing Laboratory for Communications (DSPCom), State University of Campinas (UNICAMP), 13083-970 Campinas, SP, Brazil*

[2] *Laboratory of Electronics and Communications, Conservatoire National des Arts et Métiers (CNAM), 75141 Paris, France*

Correspondence should be addressed to Danilo Zanatta Filho, daniloz@decom.fee.unicamp.br

We propose a flexible transmission scheme which easily allows to switch between cyclic-prefixed single-carrier (CP-SC) and cyclic-prefixed multicarrier (CP-MC) transmissions. This scheme takes advantage of the best characteristic of each scheme, namely, the low peak-to-average power ratio (PAPR) of the CP-SC scheme and the robustness to channel selectivity of the CP-MC scheme. Moreover, we derive the optimum power allocation for the CP-SC transmission considering a zero-forcing (ZF) and a minimum mean-square error (MMSE) receiver. By taking the PAPR into account, we are able to make a better analysis of the overall system and the results show the advantage of the CP-SC-MMSE scheme for flat and mild selective channels due to their low PAPR and that the CP-MC scheme is more advantageous for a narrow range of channels with severe selectivity.

1. INTRODUCTION

Orthogonal frequency division multiplexing (OFDM) is already used in digital radio (DAB), digital television (DVB), wireless local area networks (e.g., IEEE 802.11a/g and HIPERLAN/2), broadband wireless access (e.g., IEEE 802.16), digital subscriber lines (DSL) and certain ultra wide band (UWB) systems (e.g., MBOA). Recently, it has also been proposed for future cellular mobile systems [1]. By implementing an inverse fast Fourier transform (IFFT) at the transmitter and a fast Fourier transform (FFT) at the receiver, OFDM converts a selective channel, which presents intersymbol interference (ISI), into parallel flat subchannels, which are ISI-free, with gains equal to the channel's frequency response values. To eliminate interblock interference (IBI) between successive IFFT-processed blocks, a cyclic-prefix (CP) of length no less than the channel order is inserted at each block by the transmitter. This CP converts the linear channel convolution into circular convolution. At the receiver, the CP is discarded, which eliminates IBI. The resulting channel convolution matrix is circulant and is diagonalized by the IFFT- and FFT-matrices (see, e.g., [2]).

Although OFDM results in simple transmitters and receivers, enabling simple equalization schemes, it has some drawbacks, among which we can cite high peak-to-average power ratio (PAPR), sensitivity to carrier frequency offset, and the fact that it does not exploit the channel diversity [3] as the more important ones. To circumvent these problems, the use of a cyclic-prefixed single-carrier (CP-SC) modulation was proposed to take advantage of, on the one hand, the simplicity of the OFDM modulation and, on the other hand, the low PAPR, the frequency offset robustness, and the inherent exploitation of the channel diversity of the SC modulation.

Several works compare the performance of OFDM and CP-SC (e.g., [4–10]). It is worth mention that the long term evolution (LTE) of the universal mobile telephone system (UMTS) is considering the use of the OFDM for downlink, but CP-SC for the uplink, mainly due to PAPR issues [11], since power amplifiers have a little dynamic range and tend to saturate signals with high PAPR. These saturations are harmful to the OFDM signal and, usually, a power back-off is necessary to control the resulting nonlinear distortion introduced by the power amplifier [12].

Here, we consider that the transmitter has partial channel state information (CSI), in terms of the signal-to-noise ratio (SNR) of each subchannel. In this scenario, it is well known that for OFDM it is possible to allocate power and bits across the subchannels in order to maximize the rate [13]. This solution is the practical implementation of the water-filling approach, which maximizes the capacity of a frequency selective channel [14]. Indeed, in this case, OFDM exploits the differences in the SNR across subchannels. Hence, even without coding, the OFDM scheme is able to exploit the channel diversity, in contrast to the case of no CSI, where COFDM (coded OFDM) must be employed [15].

Building on our previous work [16], we propose a power allocation approach to CP-SC transmission, when a linear zero-forcing (ZF) or a minimum mean-square error (MMSE) receiver is used. The aim is to benefit from the channel knowledge at the transmitter while maintaining a low PAPR in order to reduce necessary power back-off, resulting in more power available for the transmission. The difference of the proposed power allocation in this work, in contrast to [7], is that here we propose power allocation schemes for the CP-SC schemes, while using a classical power allocation for OFDM, referred hereafter as cyclic-prefixed multicarrier (CP-MC) scheme. Moreover, we compare the performance of both transmission schemes taking into account the PAPR, in terms of the peak transmission power needed for a given transmit rate or on a fixed saturation rate with power back-off, in contrast to [5], where the comparison is performed taking into account the mean transmit power. Although for a wide variety of channels the CP-SC schemes outperform the CP-MC scheme, for highly selective channels the CP-MC approach leads to a better performance [16].

The main contribution of this work is that we propose a transmitter/receiver scheme for transmitting either a CP-SC or a CP-MC signal, with no changes in the transceiver structure but only changing one matrix at each side. We also show, for some simulated channels, the optimum point for switching from one scheme to the other in order to remain optimal in terms of the peak transmission power needed for a given transmit rate. Furthermore, for both strategies, we derive the optimal power allocation to maximize capacity, given a mean transmit power level.

The rest of this paper is organized as follows. Section 2 presents the proposed transmit and receiver schemes, including the generation, equalization, and the derivation of the obtained SNR for the single-carrier schemes and the multicarrier scheme. The optimum power allocation for these schemes is derived in Section 3, where we also derive the achievable bit rate obtained with this allocation. We assess the performance of each scheme in Section 4 by means of numerical simulations. Conclusions are drawn in Section 5.

Notations

Bold upper (lower, resp.) letters denote matrices (vectors, resp.); $(\cdot)^H$ denotes the Hermitian transpose (conjugate transpose); $\mathbf{A}(i, j)$ denotes the (i, j) entry of the matrix $\mathbf{A}$; and tr$\{\mathbf{A}\}$ denotes the trace of the matrix $\mathbf{A}$. We always index matrix and vectors entries starting from 1.

2. TRANSMISSION SCHEMES

The transmit scheme used in this work is shown in Figure 1. We note that this is a flexible transmit scheme in the sense that it can be used to generate a CP-SC signal as well as a CP-MC signal by changing the transmit switch matrix $\mathbf{Q}$. Moreover, this scheme also includes a power allocation matrix $\mathbf{P}$, which is responsible for allocating power to the transmit symbols carried by different subcarriers in the CP-MC case and for conforming the pulses that will carry the transmit symbols in the CP-SC case.

Figure 2 shows the receiver scheme, composed of an FFT, a linear frequency-domain equalizer $\mathbf{W}$, and the receive switch matrix. Once again, this scheme allows the reception of both waveforms by correctly choosing the receive switch matrix $\mathbf{Z}$.

In the sequel, we show how to choose $\mathbf{Q}$ and $\mathbf{Z}$ in order to generate either a CP-SC or a CP-MC signal and we also obtain the equalizer $\mathbf{W}$ for each scheme.

2.1. Single-carrier transmission

In order to generate a CP-SC signal, we use the transmit scheme shown in Figure 1, with the transmit switch matrix $\mathbf{Q}$ equal to the FFT matrix $\mathbf{F}$. The transmitted signal vector $\mathbf{x}$, before the cyclic extension, can be written as

$$\mathbf{x} = \mathbf{F}^H \mathbf{P} \mathbf{Q} \mathbf{s} = \mathbf{F}^H \mathbf{P} \mathbf{F} \mathbf{s}, \tag{1}$$

where $\mathbf{F}$ is the orthonormal[1] DFT (discrete Fourier transform) matrix of size N, $\mathbf{s}$ is the (length N) vector of transmitted symbols, and the power allocation matrix $\mathbf{P}$ is a diagonal $N \times N$ matrix.

Note that the transmit matrix given by $\mathbf{T} = \mathbf{F}^H \mathbf{P} \mathbf{F}$ is, by construction, a circulant matrix, which implies that each transmit symbol $s(n)$ is carried by a circulant-delayed version of the same transmit pulse (given by any column of $\mathbf{T}$), in exactly the same manner as in a classical SC modulation. Moreover, this is an adaptive scheme, since the transmit pulse can be changed by changing the power allocation matrix $\mathbf{P}$.

The received signal, after removing the cyclic prefix and FFT, can be written as

$$\mathbf{r} = \mathbf{F} \mathbf{H} \mathbf{F}^H \mathbf{P} \mathbf{F} \mathbf{s} + \mathbf{F} \mathbf{n}, \tag{2}$$

where $\mathbf{H}$ represents the effect of the composite channel resulting from the cascade of the analog transmission chain and the physical channel, and $\mathbf{n}$ is the additive noise vector at the receiver, assumed to be zero-mean, Gaussian, and white with power σ_n^2. Thanks to the insertion of the cyclic prefix at the transmitter and its removal at the receiver, the channel $\mathbf{H}$ is given by a circulant matrix with its first column given by the composite channel impulse response (appended by zeros

_____

[1] The orthonormal DFT matrix of size N is defined by its elements as $F(n,k) = (1/\sqrt{N})e^{-j2\pi[(k-1)(n-1)/N]}$, for $n = 1, \ldots, N$ and $k = 1, \ldots, N$, and it has the following properties $\mathbf{F}^H \mathbf{F} = \mathbf{I}$ and $\mathbf{F} \mathbf{F}^H = \mathbf{I}$.
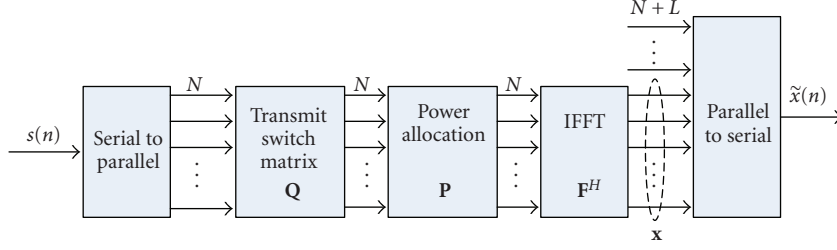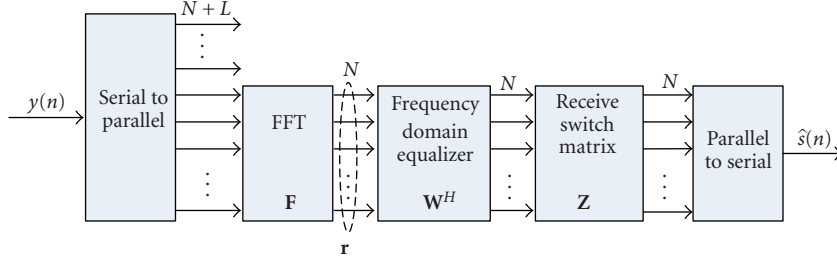
FIGURE 1: Transmit scheme.

FIGURE 2: Receiver scheme.

if needed). Recalling that the DFT matrix diagonalizes any circulant matrix [2], we can write

$$\mathbf{C} = \mathbf{F}\mathbf{H}\mathbf{F}^H, \tag{3}$$

where $\mathbf{C}$ is a diagonal matrix composed of the DFT of the composite channel impulse response, which is equivalent to the frequency response of the composite channel at the frequencies of the different subcarriers. Hence (2) simplifies to

$$\mathbf{r} = \mathbf{C}\mathbf{P}\mathbf{F}\mathbf{s} + \mathbf{F}\mathbf{n}. \tag{4}$$

In the receiver, the receive switch matrix is set to be the IFFT matrix, so that $\mathbf{Z} = \mathbf{F}^H$ and the estimated signal vector at the receiver is given by

$$\hat{\mathbf{s}} = \mathbf{F}^H\mathbf{W}^H\mathbf{r} = \mathbf{F}^H\mathbf{W}^H\mathbf{C}\mathbf{P}\mathbf{F}\mathbf{s} + \mathbf{F}^H\mathbf{W}^H\mathbf{F}\mathbf{n}, \tag{5}$$

where $\mathbf{W}$ is a diagonal $N \times N$ matrix. At this point, we are able to compute the equalizer $\mathbf{W}$. In the sequel, we analyze two different criteria to obtain this equalizer, namely the zero-forcing (ZF) criterion and the minimum mean-square error (MMSE) criterion.

2.2. ZF receiver

The ZF criterion aims to completely cancel the ISI introduced by the channel. The ZF receiver is performed by multiplying the received signal by the inverse of the overall channel in the frequency domain to compensate for the frequency selectivity, leading to an ISI-free signal at the receiver. By inspection of (5), we have that the zero-forcing equalizer is given by

$$\mathbf{W}_{\text{ZF}}^H = (\mathbf{C}\mathbf{P})^{-1} = \mathbf{P}^{-1}\mathbf{C}^{-1} = \mathbf{C}^{-1}\mathbf{P}^{-1}, \tag{6}$$

where the second equality comes from the fact that both $\mathbf{C}$ and $\mathbf{P}$ are diagonal matrices.

Using this equalizer, the estimated signal vector at the receiver reads

$$\hat{\mathbf{s}}_{\text{ZF}} = \mathbf{s} + \mathbf{F}^H\mathbf{W}_{\text{ZF}}^H\mathbf{F}\mathbf{n} = \mathbf{s} + \mathbf{F}^H\mathbf{C}^{-1}\mathbf{P}^{-1}\mathbf{F}\mathbf{n}. \tag{7}$$

The transmitted signal is then perfectly recovered (without ISI), but the noise that corrupts the decision has a covariance matrix given by

$$\mathbf{R}_{\mathbf{n}}^{\text{ZF}} = \sigma_n^2\mathbf{F}^H\mathbf{P}^{-1}\mathbf{P}^{-H}\mathbf{C}^{-1}\mathbf{C}^{-H}\mathbf{F}. \tag{8}$$

It appears that this is a circulant matrix and thus the variances of the noise (given by the diagonal elements of $\mathbf{R}_{\mathbf{n}}^{\text{ZF}}$) that corrupts each symbol in the block are the same and are given by

$$\begin{aligned}
\sigma_{n,\text{ZF}}^2 &= \sigma_n^2 \frac{1}{N}\text{tr}\{\mathbf{F}^H\mathbf{P}^{-1}\mathbf{P}^{-H}\mathbf{C}^{-1}\mathbf{C}^{-H}\mathbf{F}\} \\
&= \sigma_n^2 \frac{1}{N}\text{tr}\{\mathbf{P}^{-1}\mathbf{P}^{-H}\mathbf{C}^{-1}\mathbf{C}^{-H}\} \\
&= \sigma_n^2 \frac{1}{N}\sum_{i=1}^{N}\frac{1}{p_i c_i},
\end{aligned} \tag{9}$$

where the second equality comes from the matrix property $\text{tr}\{\mathbf{A}\mathbf{B}\} = \text{tr}\{\mathbf{B}\mathbf{A}\}$, $p_i = |\mathbf{P}(i,i)|^2$ is the power allocated to the ith subcarrier and $c_i = |\mathbf{C}(i,i)|^2$ is the squared channel gain at subcarrier i.

Hence, we can write the decision SNR for the ZF receiver as

$$\text{SNR}_{\text{ZF}} = \frac{\sigma_s^2}{\sigma_n^2}\left(\frac{1}{N}\sum_{i=1}^{N}\frac{1}{p_i c_i}\right)^{-1}, \tag{10}$$

where σ_s^2 is the power of the transmitted symbols $s(n)$.

2.3. MMSE receiver

The use of the MMSE criterion is justified by the fact that minimizing the mean-square error (MSE) leads to the maximization of the decision SNR, which is inversely proportional to the bit error rate (BER). Hence, by minimizing the MSE, one should expect to decrease the BER. The optimum MMSE solution is then given by the Wiener solution [17]

$$\mathbf{W}_{\text{MMSE}} = \mathbf{R}_{\mathbf{rr}}^{-1} \mathbf{P}_{\mathbf{rs}}, \tag{11}$$

where $\mathbf{R}_{\mathbf{rr}}$ is the correlation matrix of the received signal $\mathbf{r}$ and $\mathbf{P}_{\mathbf{rs}}$ is the cross-correlation matrix between the received signal $\mathbf{r}$ and the desired signal vector $\mathbf{s}$, where each column of $\mathbf{P}_{\mathbf{rs}}$ corresponds to the cross-correlation vector between the received signal and the respective element of the desired signal.

By using (4), we can write the correlation matrix $\mathbf{R}_{\mathbf{rr}}$ as

$$
\begin{aligned}
\mathbf{R}_{\mathbf{rr}} &= \mathrm{E}\{\mathbf{rr}^H\} \\
&= \mathrm{E}\{\mathbf{CPF}\,\mathbf{ss}^H\mathbf{F}^H\mathbf{P}^H\mathbf{C}^H\} + \mathrm{E}\{\mathbf{Fnn}^H\mathbf{F}^H\} \\
&= \sigma_s^2\mathbf{CC}^H\mathbf{PP}^H + \sigma_n^2\mathbf{I},
\end{aligned}
\tag{12}
$$

where we have used the fact that the transmitted symbols are i.i.d. with power σ_s^2, that is, $\mathrm{E}\{\mathbf{ss}^H\} = \sigma_s^2\mathbf{I}$.

The cross-correlation vector is given by

$$\mathbf{P}_{\mathbf{rs}} = \mathrm{E}\{\mathbf{rs}^H\} = \mathbf{CPF}\,\mathrm{E}\{\mathbf{ss}^H\} + \mathbf{F}\,\mathrm{E}\{\mathbf{ns}^H\} = \sigma_s^2\mathbf{CPF}, \tag{13}$$

since the noise $\mathbf{n}$ and the signal $\mathbf{s}$ are independent.

Inserting (12) and (13) into (11), we can compute the MMSE equalizer, given by

$$
\begin{aligned}
\mathbf{W}_{\text{MMSE}} &= \mathbf{R}_{\mathbf{rr}}^{-1}\mathbf{P}_{\mathbf{rs}} \\
&= \sigma_s^2\left(\sigma_s^2\mathbf{CC}^H\mathbf{PP}^H + \sigma_n^2\mathbf{I}\right)^{-1}\mathbf{CPF}.
\end{aligned}
\tag{14}
$$

We note that this equalizer depends on the channel (through its frequency response $\mathbf{C}$) and on the transmit pulse, which depends on $\mathbf{P}$.

By replacing $\mathbf{W}_{\text{MMSE}}$ in (5) with (14), the estimated symbols are given by

$$\hat{\mathbf{s}}_{\text{MMSE}} = \mathbf{As} + \mathbf{Bn}, \tag{15}$$

where $\mathbf{A} = \sigma_s^2\mathbf{F}^H\mathbf{CC}^H\mathbf{PP}^H(\sigma_s^2\mathbf{CC}^H\mathbf{PP}^H + \sigma_n^2\mathbf{I})^{-1}\mathbf{F}$ and $\mathbf{B} = \sigma_s^2\mathbf{F}^H\mathbf{P}^H\mathbf{C}^H(\sigma_s^2\mathbf{CC}^H\mathbf{PP}^H + \sigma_n^2\mathbf{I})^{-1}\mathbf{F}$.

From (15) we can compute the desired signal power and the equivalent noise and ISI power. First, let us consider only the influence of the desired signal. It appears that the gain between $\mathbf{s}$ and its estimation $\hat{\mathbf{s}}$ is given by the diagonal elements of the matrix $\mathbf{A}$, which is a circulant matrix. Hence, all diagonal elements of $\mathbf{A}$ are equal and can be written as

$$
\begin{aligned}
\mathbf{A}(i,i) &= \frac{1}{N}\mathrm{tr}\left\{\sigma_s^2\mathbf{F}^H\mathbf{CC}^H\mathbf{PP}^H\left(\sigma_s^2\mathbf{CC}^H\mathbf{PP}^H + \sigma_n^2\mathbf{I}\right)^{-1}\mathbf{F}\right\} \\
&= \frac{1}{N}\mathrm{tr}\left\{\sigma_s^2\mathbf{CC}^H\mathbf{PP}^H\left(\sigma_s^2\mathbf{CC}^H\mathbf{PP}^H + \sigma_n^2\mathbf{I}\right)^{-1}\right\} \\
&= \frac{1}{N}\sum_{i=1}^{N}\frac{\sigma_s^2 p_i c_i}{\sigma_s^2 p_i c_i + \sigma_n^2}.
\end{aligned}
\tag{16}
$$

Then, the power of the desired signal at any instant is given by

$$P_d = \sigma_s^2\left(\frac{1}{N}\sum_{i=1}^{N}\frac{\sigma_s^2 p_i c_i}{\sigma_s^2 p_i c_i + \sigma_n^2}\right)^2. \tag{17}$$

We can also compute the power of the estimated signal (P_e), defined as the power of the desired signal (P_d) plus the power of the ISI (P_{ISI}). The power of the estimated signal is given by the diagonal elements of the covariance matrix of the estimated signal, which, due to the fact that it is also a circulant matrix, is given by

$$
\begin{aligned}
P_e = P_d + P_{\text{ISI}} &= \frac{1}{N}\mathrm{tr}\{\mathrm{E}[\mathbf{Ass}^H\mathbf{A}^H]\} \\
&= \sigma_s^2\frac{1}{N}\mathrm{tr}\left\{\left[\sigma_s^2\mathbf{CC}^H\mathbf{PP}^H\left(\sigma_s^2\mathbf{CC}^H\mathbf{PP}^H + \sigma_n^2\mathbf{I}\right)^{-1}\right]^2\right\} \\
&= \sigma_s^2\frac{1}{N}\sum_{i=1}^{N}\left(\frac{\sigma_s^2 p_i c_i}{\sigma_s^2 p_i c_i + \sigma_n^2}\right)^2.
\end{aligned}
\tag{18}
$$

Finally, we can compute the power of the noise that corrupts the desired signal, given by the diagonal elements of the covariance matrix of the equivalent noise. From (15), we can write the equivalent noise covariance matrix as

$$\mathbf{R}_{\mathbf{n}}^{\text{MMSE}} = \sigma_n^2\left(\sigma_s^2\right)^2\mathbf{F}^H\mathbf{CC}^H\mathbf{PP}^H\left(\sigma_s^2\mathbf{CC}^H\mathbf{PP}^H + \sigma_n^2\mathbf{I}\right)^{-2}\mathbf{F}. \tag{19}$$

which is also a circulant matrix. Therefore, it allows to express the variance of the equivalent noise by

$$P_n = \frac{1}{N}\mathrm{tr}\{\mathbf{R}_{\mathbf{n}}^{\text{MMSE}}\} = \sigma_n^2\frac{1}{N}\sum_{i=1}^{N}\frac{\left(\sigma_s^2\right)^2 p_i c_i}{\left(\sigma_s^2 p_i c_i + \sigma_n^2\right)^2}. \tag{20}$$

Once the quantities $P_e = P_d + P_{\text{ISI}}$ and P_n have been defined, we can express the signal to signal-plus-interference-plus-noise ratio (SSINR) of the estimated signal as

$$\text{SSINR}_{\text{MMSE}} = \frac{P_d}{P_d + P_{\text{ISI}} + P_n} = \frac{P_d}{P_e + P_n}. \tag{21}$$

As shown in the appendix, this SSINR is given by

$$\text{SSINR}_{\text{MMSE}} = \frac{1}{N}\sum_{i=1}^{N}\frac{\sigma_s^2 p_i c_i}{\sigma_s^2 p_i c_i + \sigma_n^2}. \tag{22}$$

The equivalent decision SNR for the MMSE receiver is given by

$$
\begin{aligned}
\text{SNR}_{\text{MMSE}} &= \frac{\text{SSINR}_{\text{MMSE}}}{1 - \text{SSINR}_{\text{MMSE}}} \\
&= \left[\left(\frac{1}{N}\sum_{i=1}^{N}\frac{\sigma_s^2 p_i c_i}{\sigma_s^2 p_i c_i + \sigma_n^2}\right)^{-1} - 1\right]^{-1}.
\end{aligned}
\tag{23}
$$

2.4. Multicarrier transmission

To generate a CP-MC signal, we simply set the transmit switch matrix equal the identity matrix, $\mathbf{Q} = \mathbf{I}$, so that the transmit symbols $s(n)$ are directly carried by the different subcarriers, after power allocation.

The transmitted signal vector $\mathbf{x}$, before the cyclic extension, is then given by

$$\mathbf{x} = \mathbf{F}^H \mathbf{PQs} = \mathbf{F}^H \mathbf{Ps}. \tag{24}$$

The received signal, after removing the cyclic prefix and FFT, reads

$$\mathbf{r} = \mathbf{CPs} + \mathbf{Fn}. \tag{25}$$

At the receiver, we set $\mathbf{Z} = \mathbf{I}$ and the estimated signal vector is given by

$$\hat{\mathbf{s}} = \mathbf{W}^H \mathbf{r} = \mathbf{W}^H \mathbf{CPs} + \mathbf{W}^H \mathbf{Fn}. \tag{26}$$

Each subcarrier is then independently equalized by applying the gain $\mathbf{W}(i, i)^*$ at the receiver. This gain can be obtained either by using a ZF or an MMSE criterion, resulting in the same performance. So, considering the ZF criterion, we have that

$$\mathbf{W}_{\mathrm{OFDM}}^H = \mathbf{C}^{-1} \mathbf{P}^{-1}, \tag{27}$$

and the estimated signal reads

$$\hat{\mathbf{s}}_{\mathrm{OFDM}} = \mathbf{s} + \mathbf{C}^{-1} \mathbf{P}^{-1} \mathbf{Fn}. \tag{28}$$

The resulting SNR at subcarrier i is then given by

$$\mathrm{SNR}_i^{\mathrm{OFDM}} = \frac{\sigma_s^2 p_i c_i}{\sigma_n^2}. \tag{29}$$

3. POWER ALLOCATION

The goal of this section is to find the optimal power allocation matrix $\mathbf{P}$ to maximize the achievable rate subject to a constant transmit power and a given scheme. The constraint on the transmit power is related to the values of the coefficients p_i and can be expressed as

$$\sum_{i=1}^N p_i = N. \tag{30}$$

This constraint implies that the power of the transmitted signal $x(n)$ is the same of the symbols $s(n)$, given by σ_s^2. The coefficients p_i are only responsible for distributing this transmit power across the subcarriers.

In the next two sections, we derive the optimum power allocation for the CP-SC ZF and MMSE receivers obtained in Section 2, and in the following section, we consider the CP-MC case.

3.1. CP-SC-ZF scheme

For the CP-SC schemes, maximizing the achievable bit rate implies the maximization of the decision SNR. From (10) we see that, in order to maximize the SNR for the ZF receiver, we only need to minimize the term between parentheses, which is the noise enhancement inherent to the ZF receiver. Hence, we can write the power allocation problem as

$$\min_{p_i} \quad \sum_{i=1}^N \frac{1}{p_i c_i}$$
$$\text{s.t.} \quad \sum_{i=1}^N p_i = N. \tag{31}$$

This problem can be solved by the use of Lagrange multipliers. The Lagrange cost function is then given by

$$J_{\mathrm{ZF}} = \sum_{i=1}^N \frac{1}{p_i c_i} + \lambda \left(N - \sum_{i=1}^N p_i \right), \tag{32}$$

where λ is the Lagrange multiplier.

The optimum solution is obtained by setting the derivative of J_{ZF} (with respect to p_i) to zero. These derivatives are given by

$$\frac{\partial J_{\mathrm{ZF}}}{\partial p_i} = -\frac{1}{(p_i)^2 c_i} - \lambda. \tag{33}$$

And thus, by making $\partial J_{\mathrm{ZF}} / \partial p_i = 0$, we find

$$p_i = -\frac{1}{\sqrt{\lambda}} \frac{1}{\sqrt{c_i}}. \tag{34}$$

The value of λ can be computed so that the constraint of constant transmit power is respected

$$\sum_{i=1}^N p_i = -\frac{1}{\sqrt{\lambda}} \sum_{i=1}^N \frac{1}{\sqrt{c_i}} = N, \tag{35}$$

leading to

$$-\frac{1}{\sqrt{\lambda}} = N \left(\sum_{i=1}^N \frac{1}{\sqrt{c_i}} \right)^{-1}. \tag{36}$$

The optimum power allocation for the ZF receiver is then given by

$$p_i^{\mathrm{opt,ZF}} = \left(\frac{1}{N} \sum_{i=1}^N \frac{1}{\sqrt{c_i}} \right)^{-1} \sqrt{\frac{1}{c_i}}. \tag{37}$$

By replacing the optimal powers p_i in (10), we obtain the optimum decision SNR for the ZF receiver as

$$\mathrm{SNR}_{\mathrm{ZF}}^{\mathrm{opt}} = \frac{\sigma_s^2}{\sigma_n^2} \left(\frac{1}{N} \sum_{i=1}^N \frac{1}{\sqrt{c_i}} \right)^{-2}. \tag{38}$$

In possession of this SNR, we can readily obtain the achievable bit rate per transmitted symbol for the ZF receiver scheme, given by

$$C_{\mathrm{ZF}}^{\mathrm{opt}} = \log_2 \left[1 + \frac{\sigma_s^2}{\sigma_n^2} \left(\frac{1}{N} \sum_{i=1}^N \frac{1}{\sqrt{c_i}} \right)^{-2} \right]. \tag{39}$$

3.2. CP-SC-MMSE scheme

It is straightforward to see that maximizing the SNR of the estimated symbols after the MMSE receiver is equivalent to maximize the SSINR of these symbols, given by (22).

The constrained maximization of the SSINR can thus be written as

$$\max_{p_i} \quad \text{SSINR} = \sum_{i=1}^{N} \frac{\sigma_s^2 p_i c_i}{\sigma_s^2 p_i c_i + \sigma_n^2}$$
$$\text{s.t.} \quad \sum_{i=1}^{N} p_i = N, \tag{40}$$

which can also be solved by using Lagrange multipliers. The Lagrange cost function is given by

$$J_{\text{MMSE}} = \sum_{i=1}^{N} \frac{\sigma_s^2 p_i c_i}{\sigma_s^2 p_i c_i + \sigma_n^2} + \lambda \left(N - \sum_{i=1}^{N} p_i \right), \tag{41}$$

where λ is the Lagrange multiplier.

The derivative of J_{MMSE} with respect to the powers p_i is

$$\frac{\partial J_{\text{MMSE}}}{\partial p_i} = \frac{\sigma_s^2 c_i \sigma_n^2}{\left(\sigma_s^2 p_i c_i + \sigma_n^2 \right)^2} - \lambda, \tag{42}$$

and the optimum powers p_i can be found by making $\partial J_{\text{MMSE}}/\partial p_i = 0$ as follows:

$$\frac{\partial J_{\text{MMSE}}}{\partial p_i} = \frac{\sigma_s^2 c_i \sigma_n^2}{\left(\sigma_s^2 p_i c_i^2 + \sigma_n^2 \right)^2} - \lambda = 0. \tag{43}$$

After some manipulations, we can rewrite (43) as

$$p_i = \left[\frac{1}{\sqrt{\lambda}} \sqrt{\frac{\sigma_n^2}{\sigma_s^2 c_i}} - \frac{\sigma_n^2}{\sigma_s^2 c_i} \right]^+, \tag{44}$$

where $[a]^+$ is equal to a if $a \geq 0$ and is equal to 0 otherwise.

Equation (44) shows that the optimal powers p_i follow a water-filling principle [13, 14]. These optimal values can thus be obtained by adjusting the water-level $1/\sqrt{\lambda}$ to respect the power constraint and then computing the optimal powers using (44). It is important to highlight that, since we are dealing with powers, the values p_i must all be nonnegative, which explains the use of the operator $[\cdot]^+$.

If we assume that all terms between brackets in (44) are nonnegative, that is, all subcarriers are used in the transmission, we can obtain the value of λ analytically as

$$\sqrt{\lambda} = \frac{\sum_{i=l}^{N} \sqrt{\sigma_n^2/\sigma_s^2 c_i}}{N + \sum_{i=1}^{N} \left(\sigma_n^2/\sigma_s^2 c_i \right)}, \tag{45}$$

and the optimal powers read

$$p_i^{\text{opt, MMSE}} = \left(\frac{N + \sum_{i=l}^{N} \left(\sigma_n^2/\sigma_s^2 c_i \right)}{\sum_{i=l}^{N} \sqrt{\sigma_n^2/\sigma_s^2 c_i}} \right) \sqrt{\frac{\sigma_n^2}{\sigma_s^2 c_i}} - \frac{\sigma_n^2}{\sigma_s^2 c_i}. \tag{46}$$

Nevertheless, if some p_i are negative, the optimum solution is obtained by dropping the subcarriers where $p_i < 0$ and

computing (46) again for this new subset of subcarriers. This process is repeated until all powers are nonnegative and the final subset of used subcarriers is called Ω. It is worth highlighting that both summations of (46) are now carried on the subset Ω.

By using these optimal powers in (23), we obtain the optimum decision SSINR for the MMSE receiver as

$$\text{SSINR}_{\text{MMSE}}^{\text{opt}} = \frac{N_\Omega}{N} - \frac{(1/N) \left(\sum_{i \in \Omega} \sqrt{\sigma_n^2/\sigma_s^2 c_i} \right)^2}{N + \sum_{i \in \Omega} \left(\sigma_n^2/\sigma_s^2 c_i \right)}, \tag{47}$$

where N_Ω is the cardinality of Ω. Hence, after some manipulation, the achievable bit rate per transmitted symbol for the MMSE receiver scheme is given by

$$C_{\text{MMSE}}^{\text{opt}}$$
$$= \log_2 \left[\frac{N + \sum_{i \in \Omega} \dfrac{\sigma_n^2}{\sigma_s^2 c_i}}{(N - N_\Omega)\left(1 + \dfrac{1}{N} \sum_{i \in \Omega} \dfrac{\sigma_n^2}{\sigma_s^2 c_i}\right) + \dfrac{1}{N}\left(\sum_{i \in \Omega} \sqrt{\dfrac{\sigma_n^2}{\sigma_s^2 c_i}} \right)^2} \right]. \tag{48}$$

3.3. CP-MC scheme

In the case of CP-MC transmission, the optimum power allocation to maximize the achievable rate is given by the well known water-filling solution [13, 14]. Following the same algorithm for finding the subset of used subcarriers Ψ, the optimal CP-MC power allocation is given by

$$p_i^{\text{opt, CP-MC}} = \left(\frac{N}{N_\Psi} + \frac{1}{N_\Psi} \sum_{k \in \Psi} \frac{\sigma_n^2}{\sigma_s^2 c_i} \right) - \frac{\sigma_n^2}{\sigma_s^2 c_i} \quad \forall i \in \Psi, \tag{49}$$

where N_Ψ is the cardinality of Ψ.

The achievable bit rate per transmitted symbol[2] for the CP-MC scheme is given by

$$C_{\text{CP-MC}}^{\text{opt}}$$
$$= \frac{1}{N} \log_2 \left[\prod_{i \in \Psi} \frac{\left((N/N_\Psi) + (1/N_\Psi) \sum_{i \in \Psi} (\sigma_n^2/\sigma_s^2 c_i) \right) \sigma_s^2 c_i}{\sigma_n^2} \right]. \tag{50}$$

4. SIMULATION RESULTS

We consider the proposed transmit and receive schemes, shown in Figures 1 and 2, with $N = 256$ subcarriers. In order to assess the performances of the proposed technique, we consider a first-order FIR channel, described by one zero placed at α. This channel is normalized so that its energy is unitary, resulting in

$$h(z) = \frac{1 - \alpha z^{-1}}{\sqrt{1 + \alpha^2}}. \tag{51}$$

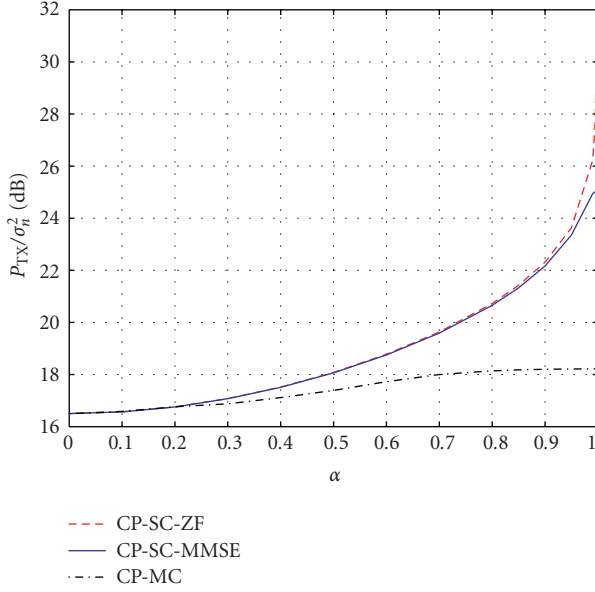[2] Here symbol denotes each one of the N samples in the block and not the global CP-MC symbol (the block itself).

FIGURE 3: Mean transmit power needed to transmit 4 bits/symbol as a function of the selectiveness of the channel α.

FIGURE 4: Complementary cumulative distribution function (ccdf) of the transmit power for 4 bits/symbol.

In the following, we first compare the performance of the single-carrier schemes (CP-SC-ZF and CP-SC-MMSE) with that of the more classical water-filled CP-MC as a function of the selectiveness of the channel, expressed by the parameter α. For each channel, we compute the optimum power allocation to achieve a given normalized rate (in bits/symbol) for a target BER of 10^{-3}. We have limited the modulation cardinality to 30 bits/symbol. We observe that the CP-MC scheme is able to achieve any rate from 0 to 30 bits/symbol, whereas the CP-SC schemes can only achieve integer rates.

In order to understand the behavior of the schemes as a function of the selectiveness of the channel, we have plotted the mean transmit power needed to transmit 4 bits/symbol as a function of the parameter α, shown in Figure 3. It is worth noting that the value of 4 bits/symbol was chosen to present the graphics, but the analysis and conclusions are the same for any other chosen value. We can see in 3 that both CP-SC schemes perform very close to the CP-MC scheme for low values of α (low selectivity) and present a power loss that increases with the parameter α. Moreover, we see that the CP-SC-ZF scheme degrades quicker than the CP-SC-MMSE for $\alpha > 0.9$ due to the noise enhancement inherent to the ZF receiver.

However, as discussed earlier, the mean transmit power is not the only performance indicator and the PAPR must be taken into account for a better analysis of the overall system performance. In order to characterize the behavior of the PAPR of each scheme, we consider the complementary cumulative distribution function (ccdf) of the transmit power for the proposed schemes, as shown in Figure 4 for some representative values of α. Note that the value of the ccdf for a given PAPR is equivalent to the probability that the transmit signal is above this PAPR, which can be seen as the probability of saturation given a back-off equal to this PAPR. We observe that both CP-SC schemes have
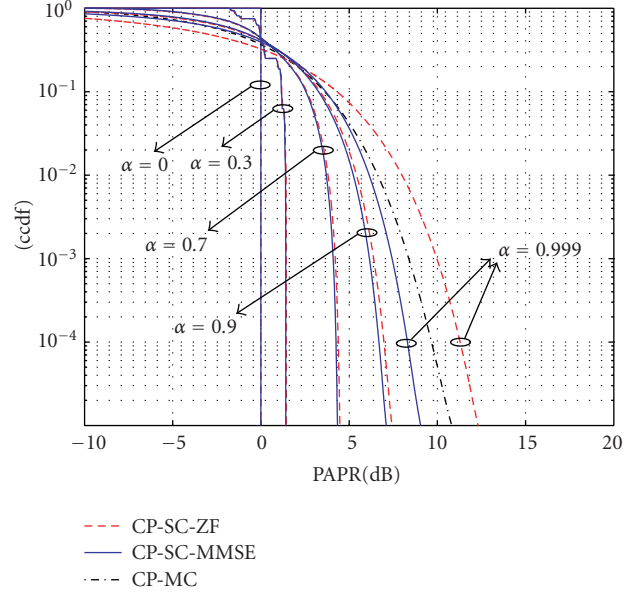
similar PAPR distribution for values of α up to 0.9, but the CP-SC-ZF scheme presents higher PAPR with high probability with respect to the CP-SC-MMSE scheme, since the CP-SC-ZF optimum power allocation generated higher allocated powers in the subcarriers with low gain. On the other hand, when compared to the multicarrier scheme, the CP-SC-MMSE scheme shows significant gains in terms of PAPR for the whole range of values of α. This gain increases when the selectiveness of the channel decreases and also when the saturation probability decreases.

Figure 5 shows the value of the PAPR as a function of the selectiveness of the channel for no saturation and a probability of saturation of 1%. We can see that, for the CP-MC scheme, the PAPR is roughly constant and does not change with the selectiveness of the channel. When we consider the maximum transmit power (the *no saturation* case), this PAPR is of 256 (24 dB), which is the size of the FFT. However, practical systems work with a given saturation rate, which is admissible without incurring in significant performance loss. If we consider a probability of saturation of 1%, the CP-MC PAPR decreases to 6.5 dB, remaining independent of α. The CP-SC schemes start from a PAPR of 0 dB for the flat channel ($\alpha = 0$) and present an increase of this PAPR as a function α, which is higher for the no saturation case, as expected. Once again, we see that the CP-SC-ZF scheme exhibits a higher PAPR than CP-SC-MMSE, being comparable or higher than that of CP-MC for high values of α. Finally, we note that the PAPR of CP-SC-MMSE is always lower than that of CP-MC for both the considered cases.

By taking the PAPR into account, Figure 6 shows the performance in terms of the peak transmit power for no saturation and a probability of saturation of 1%. We observe that the CP-MC scheme demands a roughly constant peak power, regardless of the channel selectivity and that, by allowing a probability of saturation of 1%, one
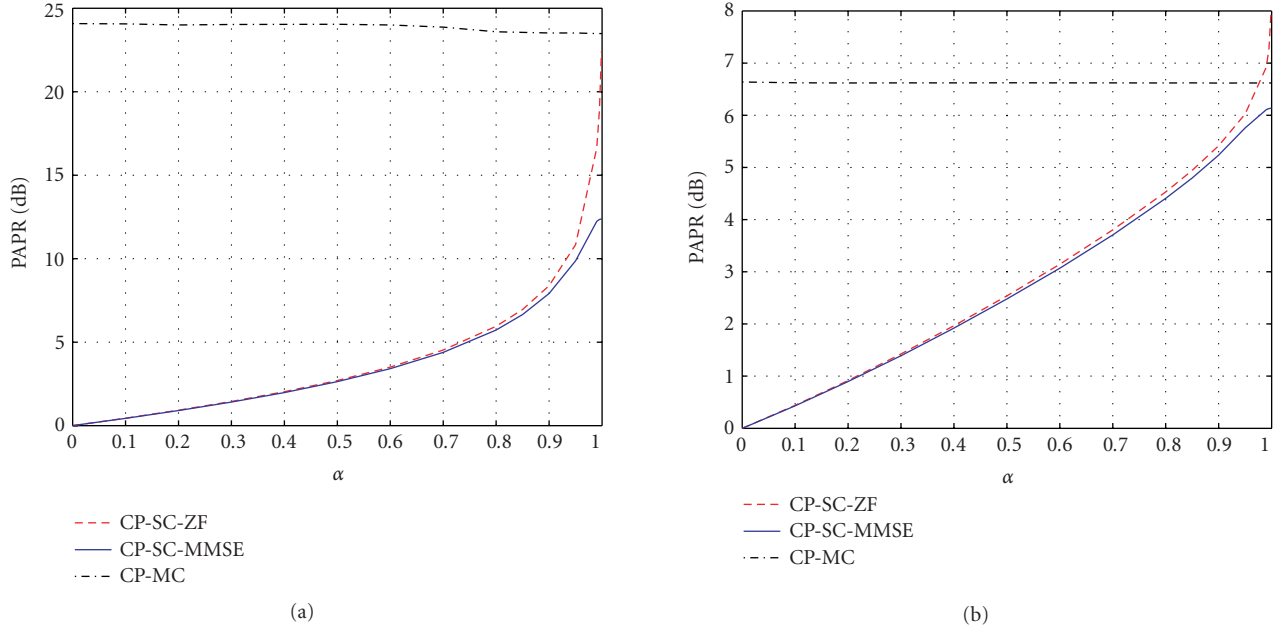
Figure 5: PAPR for (a) no saturation and (b) 1% of saturation as a function of the selectiveness of the channel α for 4 bits/symbol. Note that the PAPR-axis values are different.
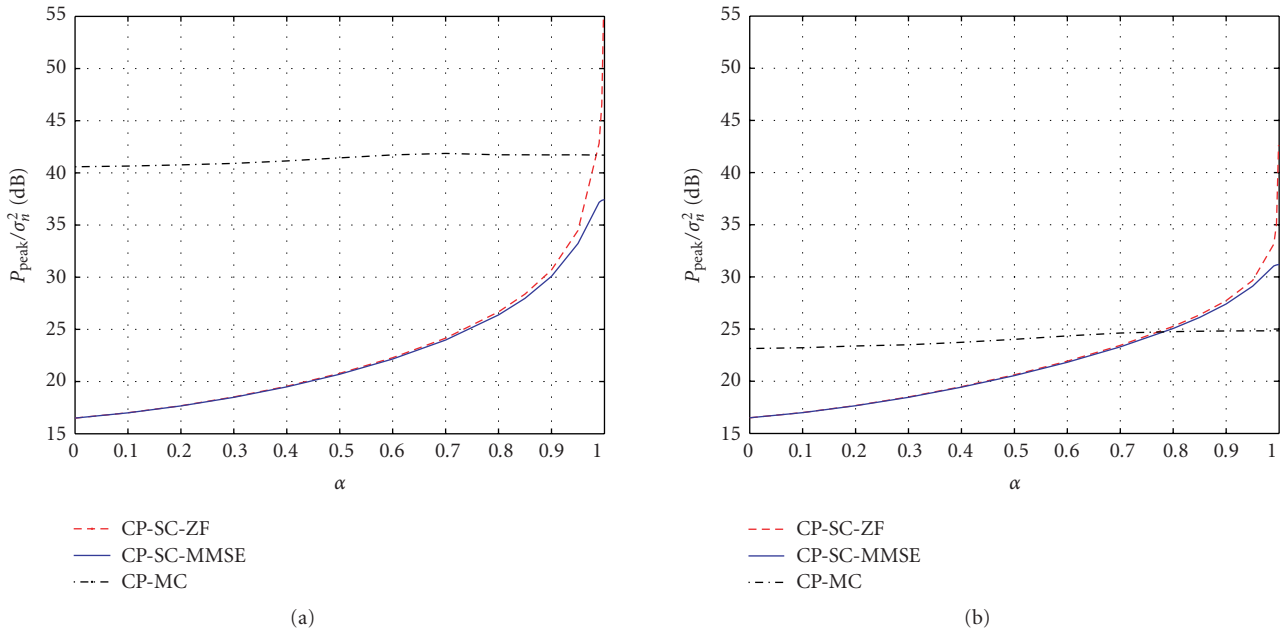

Figure 6: *Peak* transmit power needed to transmit 4 bits/symbol as a function of the selectiveness of the channel α for (a) no saturation and (b) 1% of saturation.

can gain more than 15 dB. On the other hand, the CP-SC schemes demand an exponential increase of the peak power to maintain the same transmit rate for more selective channels. This behavior comes from both the increase of the mean transmit power needed to achieve the same rate and from the increase in the PAPR for higher values of α. Nevertheless, the CP-SC schemes outperform the CP-

MC scheme for a wide range of less selective channels, that is, for the no saturation case, CP-SC-MMSE is always better than CP-MC and CP-SC-ZF is better for values of α lower than about 0.98, and for the more practical case of a probability of saturation of 1%, the CP-SC schemes are approximately equivalent, being better than CP-MC for $\alpha <$ 0.77.
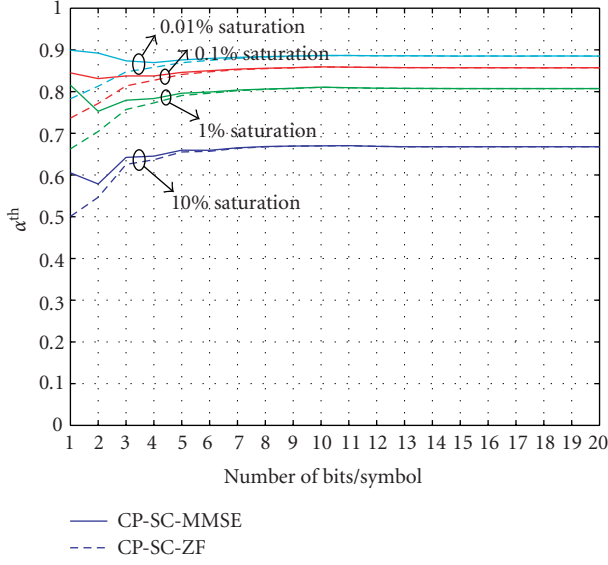
FIGURE 7: Threshold αth for switching from a single-carrier scheme to a multicarrier one as a function of the number of transmit bits/symbol and different saturation rates. Below this threshold, the CP-SC schemes outperforms the CP-MC scheme.
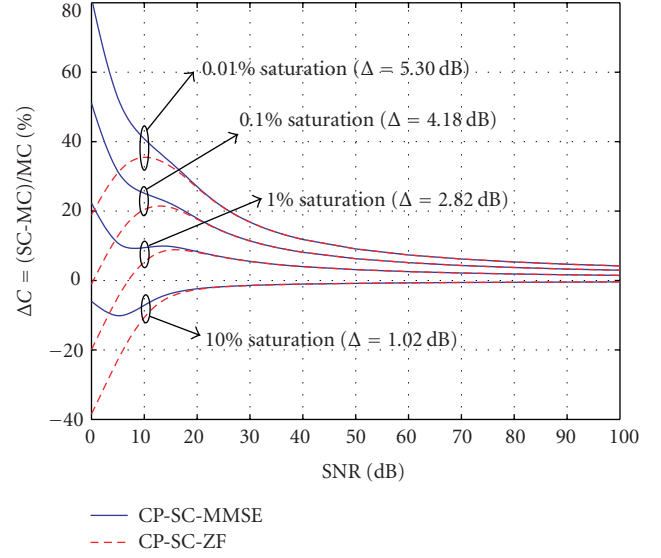

FIGURE 8: Relative capacity of the CP-SC schemes (with respect to the CP-MC scheme) as a function of the SNR for different degrees of saturation for $\alpha = 0.7$. The value between parenthesis is the differential back-off between the CP-MC scheme and the CP-SC schemes.

Hence, we see that the CP-SC schemes are advantageous over the CP-MC scheme for a wide range of channels, with the exact threshold α depending on the acceptable saturation rate. The proposed hybrid transmission scheme is based on the choice of the transmission scheme between a single-carrier and a multicarrier scheme in order to make better use of the available transmission peak power. Figure 7 shows this threshold as a function of the normalized transmit rate for different saturation rates. As expected, the CP-SC-MMSE outperforms the CP-SC-ZF scheme for small data rates and both schemes are equivalent for large data rates, since the required SNR for large data rates is high, decreasing the influence of the noise. Also, as expected, the threshold increases with the decrease of the saturation rate, favoring the CP-SC schemes over the CP-MC one. We note the asymptotic behavior of the threshold, which can be used as a rule of thumb in the design of practical systems using a hybrid transmission scheme.

4.1. Capacity results

By using the capacity results from Section 3 and the PAPR levels obtained by simulation in the first part of this section, we can now compare the achievable bit rate per transmitted symbol of the proposed schemes subject to the same saturation rates. To do so, we compute the capacity of each scheme using a suitable power back-off to respect the desired saturation rate.

Figure 8 shows the capacity of both CP-SC schemes with respect to the CP-MC scheme, in percentage, for a mild channel ($\alpha = 0.7$). We observe that, as expected from the analysis of Figure 7, the CP-SC-MMSE scheme outperforms the CP-MC one for all saturation rates except for 10%. Also, as
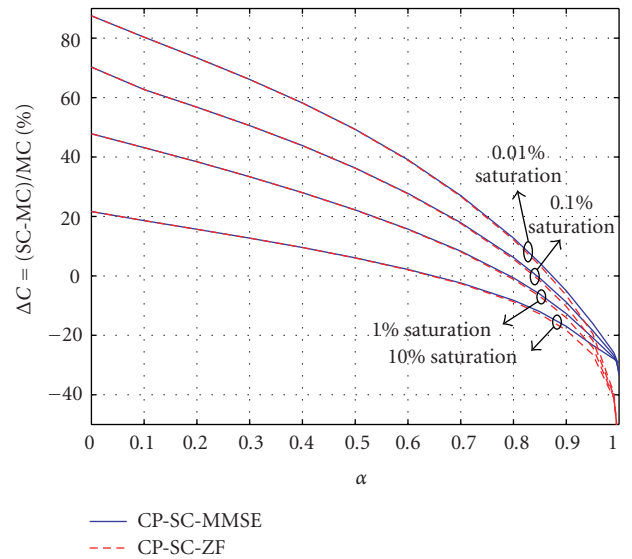
FIGURE 9: Relative capacity of the CP-SC schemes (with respect to the CP-MC scheme) as a function of the selectiveness of the channel α for an SNR of 20 dB.

expected, the CP-SC-ZF scheme performs poorly in the low SNR region due to the noise enhancement and is equivalent to the CP-SC-MMSE for high SNR. For this channel, the CP-SC-MMSE scheme achieves from 20% to more than 80% capacity gain in the low SNR region for saturation rates equal or lower than 1%. The gain for a typical application varies from 10% to 25% for 20 dB and saturation rates equal or lower than 1%. The higher gains obtained in the low SNR region are due to the fact that, in this region, the power

gain due to a lower back-off becomes more advantageous than the better immunity to selective channels of the CP-MC.

We now consider a typical condition, namely SNR of 20 dB, and assess the capacity gain as a function of the selectiveness of the channel, as shown in Figure 9. We observe gains from 20% up to 90% for flat channels by using a single-carrier scheme instead of multicarrier in this case, when taking the PAPR into account. From this figure, we can also obtain the thresholds αth for switching from one scheme to another as 0.64, 0.79, 0.84, and 0.87 for saturation rates of 10%, 1%, 0.1%, and 0.01%, respectively. We observe an agreement between these values and the asymptotic ones from Figure 7.

5. CONCLUSION

We have proposed a flexible transmission scheme which easily allows to switch between cyclic-prefixed single-carrier (CP-SC) and cyclic-prefixed multicarrier (CP-MC) transmissions by changing a matrix at the transmitter and one at the receiver. This scheme takes advantage of the best characteristic of each scheme, namely the low PAPR of the CP-SC scheme and the robustness to channel selectivity of the CP-MC scheme. Moreover, we have derived the optimum power allocation for the CP-SC transmission considering a zero-forcing (ZF) and a minimum mean-square error (MMSE) receiver. By doing so, we were able to make a fair comparison between CP-MC and CP-SC when the transmitter has partial channel state information (CSI).

By taking the PAPR into account for a better analysis of the overall system, the simulations results show the advantage of the CP-SC schemes, in particular of the CP-SC-MMSE scheme for flat and mild selective channels due to their low PAPR. On the other hand, the CP-MC scheme is more advantageous for a narrow range of channels with severe selectivity.

We have also derived the capacity of the proposed schemes with optimal power allocation. The simulation results show typical gains of about 20% to 50% when switching to the CP-SC-MMSE scheme for channels that do not present a high selectivity.

APPENDIX

From (21), the MMSE SSINR can be expressed as

$$
\text{SSINR}_{\text{MMSE}} = \frac{\sigma_s^2 \left(\dfrac{1}{N} \sum_{i=1}^{N} \dfrac{\sigma_s^2 p_i c_i}{\sigma_s^2 p_i c_i + \sigma_n^2} \right)^2}{\sigma_s^2 \dfrac{1}{N} \sum_{i=1}^{N} \left(\dfrac{\sigma_s^2 p_i c_i}{\sigma_s^2 p_i c_i + \sigma_n^2} \right)^2 + \sigma_n^2 \dfrac{1}{N} \sum_{i=1}^{N} \dfrac{\left(\sigma_s^2\right)^2 p_i c_i}{\left(\sigma_s^2 p_i c_i + \sigma_n^2\right)^2}} .
$$

(A.1)

By simplifying the term σ_s^2, we can rewrite (A.1) as follows

$$
\text{SSINR}_{\text{MMSE}} = \frac{\left(\dfrac{1}{N} \sum_{i=1}^{N} \dfrac{\sigma_s^2 p_i c_i}{\sigma_s^2 p_i c_i + \sigma_n^2} \right)^2}{\dfrac{1}{N} \sum_{i=1}^{N} \left(\dfrac{\sigma_s^2 p_i c_i}{\sigma_s^2 p_i c_i + \sigma_n^2} \right)^2 + \sigma_n^2 \dfrac{1}{N} \sum_{i=1}^{N} \dfrac{\sigma_s^2 p_i c_i}{\left(\sigma_s^2 p_i c_i + \sigma_n^2\right)^2}} .
$$

(A.2)

By converting the two terms in the denominator of (A.2) to the common denominator, we have

$$
\begin{aligned}
\text{SSINR}_{\text{MMSE}} &= \frac{\left((1/N)\sum_{i=1}^{N} \left(\sigma_s^2 p_i c_i / \sigma_s^2 p_i c_i + \sigma_n^2 \right) \right)^2}{(1/N)\sum_{i=1}^{N} \left[\left(\sigma_s^2 p_i c_i\right)^2 + \sigma_n^2 \left(\sigma_s^2 p_i c_i\right) / \left(\sigma_s^2 p_i c_i + \sigma_n^2\right)^2 \right]} \\[2mm]
&= \frac{\left((1/N)\sum_{i=1}^{N} \left(\sigma_s^2 p_i c_i / \sigma_s^2 p_i c_i + \sigma_n^2 \right) \right)^2}{(1/N)\sum_{i=1}^{N} \left[\sigma_s^2 p_i c_i \left(\sigma_s^2 p_i c_i + \sigma_n^2\right) / \left(\sigma_s^2 p_i c_i + \sigma_n^2\right)^2 \right]} \\[2mm]
&= \frac{\left((1/N)\sum_{i=1}^{N} \left(\sigma_s^2 p_i c_i / \sigma_s^2 p_i c_i + \sigma_n^2 \right) \right)^2}{(1/N)\sum_{i=1}^{N} \left(\sigma_s^2 p_i c_i / \sigma_s^2 p_i c_i + \sigma_n^2 \right)} \\[2mm]
&= \frac{1}{N} \sum_{i=1}^{N} \frac{\sigma_s^2 p_i c_i}{\sigma_s^2 p_i c_i + \sigma_n^2} .
\end{aligned}
$$

(A.3)

ACKNOWLEDGMENTS

REFERENCES

[1] Z. Wang, X. Ma, and G. B. Giannakis, "OFDM or single-carrier block transmissions?" *IEEE Transactions on Communications*, vol. 52, no. 3, pp. 380–394, 2004.

[2] P. J. Davis, *Circulant Matrices*, John Wiley & Sons, New York, NY, USA, 1979.

[3] H. Sari, G. Karam, and I. Jeanclaude, "An analysis of orthogonal frequency-division multiplexing for mobile radio applications," in *Proceedings of the 44th IEEE Vehicular Technology Conference (VTC '94)*, vol. 3, pp. 1635–1639, Stockholm, Sweden, June 1994.

[4] D. Falconer, S. L. Ariyavisitakul, A. Benyamin-Seeyar, and B. Eidson, "Frequency domain equalization for single-carrier broadband wireless systems," *IEEE Communications Magazine*, vol. 40, no. 4, pp. 58–66, 2002.

[5] J. Louveaux, L. Vandendorpe, and T. Sartenaer, "Cyclic prefixed single carrier and multicarrier transmission: bit rate comparison," *IEEE Communications Letters*, vol. 7, no. 4, pp. 180–182, 2003.

[6] H. Sari, G. Karam, and I. Jeanclaude, "Transmission techniques for digital terrestrial TV broadcasting," *IEEE Communications Magazine*, vol. 33, no. 2, pp. 100–109, 1995.

[7] N. Wang and S. D. Blostein, "Comparison of CP-based single carrier and OFDM with power allocation," *IEEE Transactions on Communications*, vol. 53, no. 3, pp. 391–394, 2005.

[8] Y. Wang, X. Dong, P. H. Wittke, and S. Mo, "Cyclic prefixed single carrier transmission in ultra-wide band communications," *IEEE Transactions on Wireless Communications*, vol. 5, no. 8, pp. 2017–2021, 2006.

[9] L. Feng and W. Namgoong, "Generalization of single-carrier and multicarrier cyclic prefixed communication," in *Proceedings of the IEEE Global Telecommunications Conference (GLOBECOM '05)*, vol. 4, pp. 2174–2178, St. Louis, Mo, USA, November-December 2005.

[10] A. Czylwik, "Comparison between adaptive OFDM and single carrier modulation with frequency domain equalization," in *Proceedings of the 47th IEEE Vehicular Technology Conference (VTC '97)*, vol. 2, pp. 865–869, Phoenix, Ariz, USA, May 1997.

[11] A. Toskala, H. Holma, K. Pajukoski, and E. Tiirola, "UTRAN long term evolution in 3GPP," in *Proceedings of the 17th IEEE International Symposium on Personal, Indoor and Mobile Radio Communications (PIMRC '06)*, pp. 1–5, Helsinki, Finland, September 2006.

[12] J. Tellado, *Multicarrier Modulation with Low PAR: Applications to DSL and Wireless*, Kluwer Academic Publishers, Boston, Mass, USA, 2000.

[13] T. Starr, J. M. Cioffi, and P. J. Silverman, *Understanding Digital Subscriber Line Technology*, Prentice-Hall, Upper Saddle River, NJ, USA, 1998.

[14] T. M. Cover and J. A. Thomas, *Elements of Information Theory*, John Wiley & Sons, New York, NY, USA, 1991.

[15] B. Le Floch, R. Halbert-Lassalle, and D. Castelain, "Digital sound broadcasting to mobile receivers," *IEEE Transactions on Consumer Electronics*, vol. 35, no. 3, pp. 493–503, 1989.

[16] D. Zanatta Filho, L. Féty, and M. Terré, "Water-filling for cyclic-prefixed single-carrier transmission and MMSE receiver," in *Proceedings of the 13th European Wireless Conference (EW '07)*, Paris, France, April 2007.

[17] S. Haykin, *Adaptive Filter Theory*, Prentice-Hall, Upper Saddle River, NJ, USA, 3rd edition, 1996.